Temporal behavior of a solute cloud in a heterogeneous porous medium 3. Numerical simulations

Marco Dentz

Department of Environmental Science and Energy Research, Weizmann Institute of Science, Rehovot, Israel

Harald Kinzelbach

Institut für Theoretische Physik, Universität Heidelberg, Heidelberg, Germany

Sabine Attinger and Wolfgang Kinzelbach

Institut für Hydromechanik und Wasserwirtschaft, Eidgenössisch Technische Hochschule Zürich, Zürich, Switzerland

Received 23 February 2001; revised 4 February 2002; accepted 4 February 2002; published 25 July 2002.

[1] The article presents systematic numerical simulations of the temporal behavior of a passive solute in a saturated three-dimensional heterogeneous medium. The groundwater flow is derived from the linearized solution of the Darcy equation with Gauss-distributed log hydraulic conductivity. The transport of a passive solute is studied by a random-walk method, which allows for a systematic study of the temporal behavior of the effective and ensemble dispersion coefficients. The numerical results are compared to the second-order perturbation theory expressions given in two companion papers [*Dentz et al.*, 2000a, 2000b] and to nonperturbative results which follow from Corrsin's conjecture. The low-order perturbation theory is intrinsically based on the assumption of small heterogeneity, while Corrsin's conjecture does not take into account certain contributions due to higher-order terms of the perturbation series. The simulations yield, for the first time, systematic quantitative information on the validity and the limitations of these analytic approximations. For increasing heterogeneities, considerable deviations from the theoretically predicted transport behavior are observed. *INDEX TERMS:* 1829 Hydrology: Groundwater hydrology; 1832 Hydrology: Groundwater transport; 1869 Hydrology: Stochastic processes; *KEYWORDS:* stochastic modeling, stochastic hydrology, numerical modeling

1. Introduction

[2] The numerical studies presented in this article complement and enhance the analytical efforts of two preceding articles [*Dentz et al.* 2000a, 2000b] (referred to as papers 1 and 2 in the following), in which we derived explicit analytical expressions for the temporal behavior of the dispersion coefficients for a solute plume in a heterogeneous saturated medium. As is well known from field studies and numerical simulations the transport in this case is determined by the large scale fluctuations of the physical and chemical properties of the medium. During the last decade, the stochastic modeling approach has proven to be an invaluable tool in order to quantify the influence of these spatial heterogeneities on the macroscopic transport parameters. In this approach an aquifer is assumed to be a single typical realization of an ensemble of aquifers with given statistical properties. The observables under consideration are defined as appropriate averages over the ensemble of all realizations of the medium.

[3] Our focus lies on the center of mass velocity of the solute plume and on the macroscopic dispersion coefficients. In the stochastic approach, we distinguish between two conceptually different dispersion quantities: The "effective" dispersion coefficient $D_{ij}^{\mathrm{eff}}(t)$, which measures the spreading of a plume in one typical realization and the "ensemble" dispersion coefficient $D_{ij}^{\mathrm{ens}}(t)$, which reflects the dispersion properties of the ensemble of all realizations. The fundamental difference between these quantities is well known in literature and discussed extensively by *Attinger et al.* [1999] and paper 1, where one also finds an exhaustive discussion of the relevant literature.

[4] In papers 1 and 2 we investigated the temporal behavior of the effective and ensemble dispersion coefficients in the framework of a second-order perturbation theory. In general, the second-order approach has proven to be a valuable method for the prediction of transport properties in heterogeneous porous media, see, e.g., the textbooks by *Dagan* [1989] and *Gelhar* [1993]. Nevertheless, it leaves important questions open. The longitudinal macrodispersion coefficient derived in the perturbational framework fits very well with field findings, [e.g., *Freyberg*, 1986], whereas the transverse dispersion coefficient underestimates experimental data by at least one order of magnitude [e.g., *Gelhar and Axness*, 1983]. Furthermore, since the second-order approach is based on the assumption of moderate heterogeneity, it is unclear to what extent its

Copyright 2002 by the American Geophysical Union.
0043-1397/02/2001WR000436$09.00

results remain applicable in the case of (realistic) strongly heterogeneous media. Limitations of the approach are indicated by the field experiments performed at the highly heterogeneous aquifer at the Columbus Air Force Base, U.S. [*Adams and Gelhar*, 1992]. The numerical simulations presented here are a systematic tool in order to investigate the relevance of higher-order contributions of the perturbation series to the transport coefficients. We focus on a systematic numerical investigation of the temporal behavior of the ensemble and effective dispersion coefficients. The numerical findings are compared with the second-order perturbation theory results of paper 1 and 2, and results derived from what is called "Corrsin's conjecture" in the literature [e.g., *Dagan*, 1988; *Neuman and Zhang*, 1990; *Zhang and Neuman*, 1990; *Zhang*, 1995; *Dentz*, 2000].

[5] In paper 1 we identified two different relevant timescales: The advective timescale $\tau_u = l/\overline{u}$, which dominates the time evolution of the ensemble dispersion coefficients, and the much larger dispersive time scale $\tau_D = l^2/D$, which rules the temporal behavior of the effective dispersion coefficients. According to *Gelhar and Axness* [1983] in realistic situations the ratio τ_D/τ_u is of order 10^2 to 10^4. To achieve conclusive results, the times reached in the simulations have to be at least of the order of the (large) dispersive scale. This actually is one of the severe difficulties one encounters when performing numerical simulations for the quantities under consideration. It is also the main reason why the numerical results found in the published literature sometimes are not completely conclusive.

[6] To solve the full transport problem in general implies to solve Darcy's equation for a medium with a given random permeability field [e.g., *Ababou et al.*, 1989; *Tompson and Gelhar*, 1990] and, in a second step, use the resulting flow field as an input for the advection-dispersion equation, which describes the transport process [e.g., *Burr and Sudicky*, 1994; *Naff et al.*, 1998]. Both steps are numerically demanding and, as a result, numerical investigations which try to carry out both parts without further approximations usually are limited to a few disorder realizations only, and to observation times of only a few advective timescales. The studies by *Burr and Sudicky* [1994] for a $d = 3$ dimensional model and by *Naff et al.* [1998] in $d = 2$ dimensions are based on this approach and, accordingly, suffer from these limitations. Nevertheless, they for the first time directly observed that the ensemble dispersion coefficients actually overestimates the dispersion coefficients in the single realizations, an effect which they correctly traced back to the artificial effect of plume centroid dispersion as discussed, for example, by *Attinger et al.* [1999] and paper 1. Starting from a simplified approach for the flow field, *Kapoor and Kitanidis* [1996] investigated concentration fluctuations in a two dimensional periodic porous medium. They solved the advection-dispersion equation for a flow given by the linearized solution of the Darcy equation.

[7] If one, more modestly, aims at the first two moments of the solute cloud only instead of the full concentration distribution, it appears to be more effective to describe the transport of a solute by a random-walk method. Many of the numerical investigations found in the literature use this approach. For the $d = 2$ dimensional numerical simulations by *Rubin* [1990] the flow field was given by the linearized solution of the Darcy equation. Disregarding local dispersion, he determined the ensemble dispersion coefficients. *Bellin et al.* [1992], *Salandin and Fiorotto* [1998], and *Zhang and Lin* [1998] analyzed the temporal behavior of the ensemble dispersion coefficients in the absence of local dispersion in $d = 2$ dimensions, and *Chin and Wang* [1992] did the same in $d = 3$ dimensions. The largest observation times reached are of the order of ten advection timescales. The flow field in these studies was derived by numerically solving Darcy's equation. The studies mainly confirmed the results derived from a second-order perturbation theory in the case of no local dispersion and concluded that the corresponding theoretical prediction provides a robust description of the simulation data. The role of a finite local dispersion was investigated by *Smith and Schwartz* [1980] for $d = 2$ dimensions, and *Tompson and Gelhar* [1990] for $d = 3$. Since including local dispersion effects requires an additional average over a white noise ensemble, their studies again are limited to small observation-times and a few disorder realization only. *Jaekel and Vereecken* [1997] studied the long time limit of the effective dispersion coefficients of a solute which is transported in a flow field given by the linearized solution of the Darcy equation in $d = 3$ dimensions. Even though their observation times are large compared to those of other numerical investigations found in the literature, they still are small compared to the relevant dispersive timescales. Thus their simulations do not reach the true asymptotic values. None of these studies provides a systematic investigation of the effective and ensemble dispersion coefficients. Recently *Schwarze et al.* [2001] studied the temporal behavior of a dispersion quantity which in the long time limit coincides with the long time value of the effective dispersion coefficient. In their two- and three-dimensional numerical simulations they reach observation times which are of the order of the dispersive timescale τ_D.

[8] The numerical investigations presented in this article are based on a random-walk method. The flow field is given by the simplified linearized solution of the Darcy equation. The Gaussian log hydraulic conductivity is realized as a superposition of a large number of randomly chosen harmonic modes following the method introduced by *Kraichnan* [1970] and *Kraichnan* [1976]. Using this simplified model we are able to perform efficient simulations combining long observation times with a large number of disorder realizations. Our systematic investigations of the temporal behavior and the asymptotic long-time values of the longitudinal and transverse dispersion coefficients shed some new light on the validity of the perturbational approach and Corrsin's conjecture.

2. Basics

2.1. Flow

[9] The flow field used for the transport simulations is derived from the linearized solution of the Darcy equation. According to *Gelhar and Axness* [1983], $\mathbf{u}(\mathbf{x})$ is given by

$$\mathbf{u}(\mathbf{x}) = \bar{\mathbf{u}} - \bar{u} \int \frac{\mathrm{d}^3 k}{(2\pi)^3} \exp(-\mathrm{i}\,\mathbf{k}\cdot\mathbf{x})\ \mathbf{p}(\mathbf{k})\,\tilde{f}(\mathbf{k}), \qquad (1)$$

where $\tilde{f}(\mathbf{k})$ denotes the Fourier transform of the fluctuating part of the log hydraulic conductivity $f(\mathbf{x})$. The spatially varying $\mathbf{u}(\mathbf{x})$ is split into a constant part $\bar{\mathbf{u}}$ and a random fluctuation $\mathbf{u}'(\mathbf{x})$ about this value, which is defined by the second term on the right side of equation (1). Without loss of generality, the mean flow is aligned with the 1-direction of the coordinate system:

$$\bar{\mathbf{u}} = \bar{u}\,\mathbf{e}_1, \tag{2}$$

where $\mathbf{e}_1$ is the unit vector in 1-direction. The vector $\mathbf{p}(\mathbf{k})$ ensures the incompressibility of $\mathbf{u}(\mathbf{x})$, i.e., $\nabla \cdot \mathbf{u}(\mathbf{x}) = 0$; it is defined by

$$\mathbf{p}(\mathbf{k}) \equiv \left(\mathbf{e}_1 - \frac{\mathbf{k}\,k_1}{k^2}\right). \tag{3}$$

The autocorrelation functions of the components of the flow field then read according to *Gelhar and Axness* [1983]:

$$\overline{u_i'(\mathbf{x})u_j'(\mathbf{x}')} = \bar{u}^2 \int \frac{\mathrm{d}^3k}{(2\,\pi)^3} \exp\left(-\mathrm{i}\,\mathbf{k}\cdot(\mathbf{x}-\mathbf{x}')\right) p_i(\mathbf{k})\, p_j(\mathbf{k})\, \tilde{C}(\mathbf{k}). \tag{4}$$

The overbar, as usual, stands for the average over the ensemble of permeability fields. The function $\tilde{C}(\mathbf{k})$ is the autocorrelation spectrum of the log hydraulic conductivity $f(\mathbf{x})$. The approach is mathematically well defined subject to some additional mathematical requirements for $C(\mathbf{x})$, which are summarized, for example, in the work of *Gelhar* [1993]. The particular functional form of $C(\mathbf{x})$ is to some extent arbitrary. Reflecting the situation in a heterogeneous medium, $C(\mathbf{x})$ should drop to zero sharply for lenghts larger than the intrinsic correlation length scales l_i. A convenient choice for $C(\mathbf{x})$ made in the literature is a Gauss-shaped function, see also paper 1. Thus the auto-correlation spectrum $\tilde{C}(\mathbf{k})$ is given by:

$$\tilde{C}(\mathbf{k}) = \sigma^2\,(2\pi)^{3/2} \prod_{i=1}^{3} l_i\, \exp\left(-\frac{1}{2}(k_i\,l_i)^2\right), \tag{5}$$

where the variance σ^2 measures the strength of the heterogeneities.

[10] In our simulations, the log hydraulic conductivity is generated as a superposition of randomly chosen harmonic modes as discussed by *Kraichnan* [1970, 1976]:

$$f(\mathbf{x}) = \sigma\sqrt{\frac{2}{N}} \sum_{j=1}^{N} \cos(\mathbf{k}^{(j)}\cdot\mathbf{x} + \varphi^{(j)}). \tag{6}$$

The vectors $\mathbf{k}^{(j)}$ and the phases $\varphi^{(j)}$ are independent random numbers. Their distributions determine the autocorrelation function of the resulting random field $f(\mathbf{x})$. In order to generate the autocorrelation spectrum (autocorr), the $k_i^{(j)}$ are drawn from a Gaussian distribution with vanishing average and variance $1/l_i^2$. The phases $\varphi^{(j)}$ are equally distributed in the interval $[0, 2\pi]$. In the limit $N \to \infty$, due to the Central Limit Theorem, $f(\mathbf{x})$ is a Gaussian distributed random field characterized by the autocorrelation spectrum (5). Inserting the Fourier transform of (6) into (1), we obtain for the components of the corresponding velocity field:

$$u_i(\mathbf{x}) = \bar{u}\delta_{i1} - \sigma\bar{u}\sqrt{\frac{2}{N}} \sum_{j=1}^{N} p_i(\mathbf{k}^{(j)})\, \cos(\mathbf{k}^{(j)}\cdot\mathbf{x} + \phi^{(j)}). \tag{7}$$

In the limit $N \to \infty$, $\mathbf{u}(\mathbf{x})$ is also a Gaussian random field and the auto-correlation functions of the components of $\mathbf{u}(\mathbf{x})$ are given by (4). Note that $\mathbf{u}(\mathbf{x})$ is an incompressible Gaussian distributed random field; the incompressibility is insured by the $\mathbf{p}(\mathbf{k})$, (3), and can be verified by inspection. For the numerical simulations, we used a number of $N = 64$ random modes. Using a larger number of random modes considerably increases the computation time. However, we convinced ourselves by using random flow fields $\mathbf{u}(\mathbf{x})$, (7), generated by $N = 100$, 500, and $N = 1000$ modes that the simulation results for the macrodispersion coefficients do not change.

2.2. Transport: Lagrangian Framework

[11] In contrast to the Eulerian framework [see, e.g., *Dagan*, 1989; *Gelhar*, 1993], in which the transport of a solute is given by the time evolution of its concentration distribution, the Lagrangian framework aims at the motion of solute particles. For the given transport model both representations are strictly equivalent. For a proof see any standard textbook on stochastic processes [e.g., *Risken*, 1984; *Honerkamp*, 1994]. The movement of a solute particle is determined by the flow field $\mathbf{u}(\mathbf{x})$ and a stochastic force $\boldsymbol{\xi}(t)$, which models the erratic motion of the particle due to local dispersion. The equation of motion of a solute particle reads [*Dagan*, 1989]

$$\frac{\mathrm{d}}{\mathrm{d}t}\mathbf{x}(t) = \mathbf{u}(\mathbf{x}(t)) + \boldsymbol{\xi}(t), \tag{8}$$

where $\boldsymbol{\xi}(t)$ represents a three-dimensional Gaussian white noise defined by

$$\langle \xi_i(t) \rangle = 0 \tag{9}$$

$$\left\langle \xi_i(t)\xi_j(t') \right\rangle = 2\,D_{ij}\,\delta_{ij}\,\delta(t-t') \tag{10}$$

with D_{ij} being the components of the local dispersion tensor, which in the following is assumed to be constant and diagonal. It has a longitudinal component D_L in flow direction, and transversal components D_T perpendicular to it. The angular brackets, $\langle \ldots \rangle$, denote the average over the realizations of the white noise $\boldsymbol{\xi}(t)$.

[12] In realistic situations the advective transport of the solute particles by the flow field $\mathbf{u}(\mathbf{x})$ is much more effective than the transport by local dispersion. As it turned out in the numerical simulations, it is essential to construct accurate numerical solutions of the single particle path lines to adequately take into account the influence of the spatial heterogeneities of the flow field. In order to achieve the necessary increased accuracy, we use an extended Runge-Kutta method described by *Drummond et al.* [1984] ("extended" because it accounts also for local dispersion) instead of the common Euler-method which follows from a straightforward time discretization of equation (8). The accuracy of the extended Runge-Kutta scheme is of order $(\Delta t)^{3/2}$.

[13] Within the Lagrangian framework the (Eulerian) concentration distribution $g(\mathbf{x}, t)$ is given by

$$g(\mathbf{x}, t) = \left\langle \delta^{(3)}(\mathbf{x} - \mathbf{x}(t)) \right\rangle, \tag{11}$$

where $\delta^{(3)}(\mathbf{x})$ denotes the delta-distribution in $d = 3$ dimensions. The position $\mathbf{x}(t)$ of a solute particle at time t for a given realization of the flow and the white noise follows implicitly from equation (8) [e.g., *Risken*, 1984; *Honerkamp*, 1994].

[14] Using equation (11), it is easy to translate from one framework to the other. The macroscopic center of mass velocity and the macroscopic dispersion coefficients, defined in paper 1 starting from the Eulerian framework, now read

$$u_i^{\mathrm{eff}}(t) = \frac{\mathrm{d}}{\mathrm{d}t}\overline{\langle x_i(t)\rangle} \tag{12}$$

$$D_{ii}^{\mathrm{eff}}(t) = 1/2\frac{\mathrm{d}}{\mathrm{d}t}\left\{\overline{\langle x_i(t)\, x_i(t)\rangle} - \overline{\langle x_i(t)\rangle\langle x_i(t)\rangle}\right\} \tag{13}$$

$$D_{ii}^{\mathrm{ens}}(t) = 1/2\frac{\mathrm{d}}{\mathrm{d}t}\left\{\overline{\langle x_i(t)\, x_i(t)\rangle} - \overline{\langle x_i(t)\rangle}\quad\overline{\langle x_i(t)\rangle}\right\}. \tag{14}$$

Note the order of the two ensemble averages involved. The angular brackets denote the average over the white noise $\boldsymbol{\xi}(t)$, which generates the local dispersion, the overbar stands for the average over the ensemble of possible realizations of the flow field $\mathbf{u}(\mathbf{x})$ generated by the heterogeneous medium.

2.3. Corrsin's Conjecture

[15] The are various efforts in order to solve the given transport problem approximately. The standard low-order perturbation theory is discussed at length, e.g., in paper 1.

[16] To take into account higher-order corrections, a self-consistent resummation method based on what is called "Corrsin's conjecture" is well known in the literature. Based on this approach, *Neuman and Zhang* [1990], *Zhang and Neuman* [1990], *Dagan* [1994], and *Zhang* [1995] give expressions for the ensemble dispersion coefficients within a Lagrangian framework. The approach is easily translated to an Eulerian framework using relation (11) [e.g., *Dentz*, 2000]. In a first step one gets (in d spatial dimensions)

$$D_{ii}^{\mathrm{ens}}(t) = D_{ii} + \int \frac{\mathrm{d}^d k'}{(2\pi)^d}\int \frac{\mathrm{d}^d k''}{(2\pi)^d}\int_0^t \overline{\tilde{u}_i'(\mathbf{k}')\tilde{u}_i'(\mathbf{k}'')\tilde{g}(-\mathbf{k}'', t')}, \tag{15}$$

where $\tilde{g}(\mathbf{k}, t) = \int \mathrm{d}^d x\, g(\mathbf{x}, t)\exp(\mathrm{i}\mathbf{k}\cdot\mathbf{x})$ is the spatial Fourier-transform of the concentration distribution, and $\tilde{\mathrm{u}}_i'(\mathbf{k}')$ the analog transform of the the flow field. Corrsin's Conjecture basically assumes that for large times all direct correlations between $\tilde{g}(\mathbf{k}, t)$ and $\tilde{\mathbf{u}}'(\mathbf{k})$ vanish, and that the transport becomes normal in the limit of large times. These assumptions lead to a system of self-consistent nonlinear equations:

$$D_{ii}^{\mathrm{ens}}(t) = D_{ii} + \int \frac{\mathrm{d}^d k'}{(2\pi)^d}\int \frac{\mathrm{d}^d k''}{(2\pi)^d}\int_0^t \overline{\tilde{u}_i'(\mathbf{k}')\,\tilde{u}_i'(\mathbf{k}'')}\quad\overline{\tilde{g}(-\mathbf{k}'', t')}, \tag{16}$$

with

$$\overline{\tilde{g}(\mathbf{k}, t)} = \exp\left(-D\,\mathbf{k}^2 t + \mathrm{i}\bar{u}t - \int_0^t \mathrm{d}t'\,\mathbf{k}\,\mathbf{D}^{\mathrm{ens}}(t')\,\mathbf{k}\right), \tag{17}$$

which can be solved numerically to determine the dispersion coefficients. Of course, at this point it is not clear if this resummation scheme is consistent since possible persistent cross-correlations between $\tilde{g}(\mathbf{k}, t)$ and $\tilde{\mathbf{u}}'(\mathbf{k})$ are neglected [e.g., *Dagan*, 1994; *Dentz*, 2000]. In the following, we compare the results derived from the low-order perturbation theory of paper 1 and 2, and the results from the numerical solution of equation (16) with findings from a direct numerical solution of the transport model using a random walk approach.

2.4. Setup of the Simulations

[17] Setting up the framework for the numerical simulations, we have to take into account the following criteria: (1) Since we study the temporal behavior of $\mathbf{D}^{\mathrm{ens}}(t)$ and $\mathbf{D}^{\mathrm{eff}}(t)$, we have to consider large observation times which are at least of the order of the (large) dispersive timescale τ_{D}. (2) In order to resolve the dominant influence of the spatial heterogeneity accurately we have to use a sufficiently fine time discretization interval Δt. (3) In order to resolve the effects of the local dispersion with sufficient accuracy it is necessary to use an adequate number of white noise realizations. (4) In order to suppress large sample to sample fluctuations it is necessary to consider a large number of realizations of the random flow field $\mathbf{u}(\mathbf{x})$. The simulations to determine the asymptotic values of the dispersion coefficients are performed using 2000 realizations of the flow field $\mathbf{u}(\mathbf{x})$, and 100 realizations of the temporal stochastic process $\boldsymbol{\xi}(t)$. The time is discretized as $\Delta t = 0.05\ \tau_{\mathrm{u}}$. The observation time varies between 500 τ_{u} and 1500 τ_{u}, depending on the time needed by the ensemble dispersion coefficients to become asymptotic. To evaluate the asymptotic long-time behavior we exploit the fact that the ensemble dispersion coefficients reach their final value at shorter timescales than the effective dispersion coefficients, see paper 1. Therefore we determine the asymptotic dispersion coefficients from the ensemble quantity. In order to reduce statistical fluctuations, the asymptotic value is evaluated as the average over values of $D_{ii}^{\mathrm{ens}}(t)$ in the time interval where it has already reached its final value. The statistical error of the observables given as error bars in the results below is defined as the root-mean squared deviation from this average.

[18] For the simulations investigating the temporal behavior of the ensemble and effective dispersion coefficients, we use 150 realizations of the Gaussian random process $\boldsymbol{\xi}(t)$ and 2500 realizations of the random flow field $\mathbf{u}(\mathbf{x})$. In this case, the time steps are given by $\Delta t = 0.1\ \tau_{\mathrm{u}}$ and the observation time is $t = 1000\ \tau_{\mathrm{u}}$. The observed temporal fluctuations of the observables are a consequence of the finite number of disorder realizations. These fluctuations decrease with increasing number of realizations of $\mathbf{u}(\mathbf{x})$ and $\boldsymbol{\xi}(t)$. The number of realizations of $\mathbf{u}(\mathbf{x})$ and $\boldsymbol{\xi}(t)$ as well as the time discretization Δt are limited by the computer time available.

3. Disorder-Induced Contributions to the Transport Coefficients

[19] We investigate the transport properties of a three-dimensional model with isotropic disorder correlation, $l_1 = \ldots = l_d = l$, and isotropic local dispersion, $D_L = D_T = D$, starting from a point-like injection. Additionally, we deal with an anisotropic model inspired by the characteristics of the aquifer at the Borden Site (Ontario, Canada). For the

simulations of the isotropic model we use a value of $\overline{u} = 1$ m/d for the mean flow velocity and a correlation length of $l = 1$ m. In the case of the Borden scenario, we use the data summarized in paper 1 and 2.

[20] The center of mass velocity of the plume actually does not have any disorder-induced contributions. We find $u_i^{\text{eff}}(t) = \overline{u}\ \delta_{i1}$ confirming the result of *Dagan* [1984] and paper 1. The macroscopic dispersion in contrast is influenced significantly by the spatial disorder. In the following, we systematically investigate the asymptotic behavior of the longitudinal and transverse dispersion coefficients as a function of the disorder-correlation strength σ^2 and a varying local dispersion coefficient D and compare the results with those derived from the second-order treatment of paper 1, and from Corrsin's conjecture (see section 2.3 and, e.g., *Zhang* [1995] and *Dentz* [2000]). We also analyze the temporal behavior of the effective and ensemble dispersion coefficients and compare the results with those of the perturbation theory expressions derived in paper 1, which for the first time explicitly demonstrated the significant quantitative difference between these quantities.

3.1. Asymptotic Behavior

3.1.1. Dependence on the variance

[21] Here we investigate the behavior of the asymptotic longitudinal and transverse dispersion coefficients as a function of the disorder variance σ^2. The simulations were performed for a (realistic) local dispersion coefficient of $D = 0.001$ m^2/d [*Gelhar and Axness*, 1983]. Figure 1a shows the simulation results for the longitudinal asymptotic dispersion coefficient and the corresponding behavior as predicted by perturbation theory and by Corrsin's conjecture (section 2.2.1 and *Zhang* [1995] and *Dentz* [2000]). In the case of small σ^2 the results from second-order perturbation theory as well as from Corrsin's conjecture agree well with the simulation data. For increasing σ^2, however, we observe systematic deviations. The longitudinal dispersion coefficient is larger than that predicted by both analytical approaches, which yield essentially the same results within the given range of σ^2-values.

[22] For the transverse dispersion coefficient shown in Figure 1b the situation is similar. The results from the perturbation approach and Corrsin's conjecture are almost identical and agree with the simulation data in the case of small σ^2. For increasing variances, the transverse dispersion coefficient starts to deviate from the values predicted by both the second-order perturbation theory and Corrsin's conjecture. One observes a macroscopic value for the transverse dispersion with increasing σ^2, which indicates the importance of higher-order contributions in this case. Even though the self-consistent method predicts macroscopic contributions to the transverse dispersion coefficient, it actually overestimates the simulation results considerably.

3.1.2. Dependence on the local dispersion coefficient

[23] The following subsection gives the $d = 3$ simulation results for the asymptotic dispersion coefficients as a function of the local dispersion for given (realistic) disorder variances $\sigma^2 = 0.1$ and $\sigma^2 = 1$. The simulation results again are compared with the second-order results from paper 1 and those from Corrsin's conjecture. Figure 2a shows the asymptotic longitudinal dispersion coefficient as a function of the local dispersion for $\sigma^2 = 0.1$. The results from Corrsin's conjecture and from the second-order perturbation theory do not differ considerably, and both agree well with the given simulation data. The transverse dispersion coefficient, Figure 2b, too, is described fairly well by the analytical approaches for small disorder correlation, apart from some systematic deviations for very small values of the local dispersion. These small deviations, however, already indicate the relevance of higher-order corrections. With increasing variance the second-order treatment underestimates the longitudinal as well as the transverse dispersion coefficients for a small local dispersion coefficient as shown for $\sigma^2 = 1$ in Figures 3a and 3b, respectively. The discrepancy from the behavior predicted by both analytical approaches is even more pronounced in the case of the transverse coefficient, Figure 3b. There the second-order approach predicts a value of the order of the local dispersion (i.e., negligibly small), whereas the simulations yield macroscopically large values. The latter behavior is captured at least qualitatively by Corrsin's conjecture, which, however, overestimates the simulation data. Again, the simulation results indicate the importance of higher-order contributions to the macroscopic dispersion coefficients for increasing disorder strengths. For (unrealistically) large values of the local dispersion coefficient both the transverse and the longitudinal macroscopic dispersion coefficients agree well with the perturbation theory results and Corrsin's conjecture. This, however, is not very surprising since in this limit the local dispersion is the dominant spreading mechanism, and the effects due to spatial disorder become negligible.

[24] Even though they underestimate the simulation results for $\sigma^2 = 1$, the analytic approximations capture the behavior of the longitudinal dispersion coefficient qualitatively quite well, see Figure 3a. The simulations as well as the theories indicate a nonmonotonous dependence of the longitudinal dispersion coefficient on the local dispersion coefficient D. For small values of D they first decrease with increasing D, for large values of D they increase with increasing D. This on the first sight somewhat counterintuitive behavior has already been observed by *Fiori* [1996]. It can be explained by the strong influence of the heterogeneous structure of the streamlines of the flow field on the spreading of the solute [*Dentz*, 2000].

3.2. Temporal Behavior

[25] In the following, we investigate the temporal behavior of the ensemble and the effective dispersion coefficients for a plume evolving from a point-like injection at time $t = 0$. The mean flow velocity of $\overline{u} = 1$ m/d and the isotropic disorder correlation length of $l = 1$ m imply an advective timescale of $\tau_u = l/\overline{u} = 1$ d. The dispersive timescale is given by $\tau_D = l^2/D = 100\ \tau_u$ since the local dispersion is set to $D = 0.01$ m^2/d. The chosen parameters are of the order of magnitude found in realistic aquifer situations [see, e.g., *Gelhar and Axness*, 1983]. As already discussed in paper 1, the stochastic approach has only a formal meaning for times small compared to the advective timescale τ_u. For this reason, in the following we will focus on times larger than the advective timescale $t \geq \tau_u$.

3.2.1. Longitudinal dispersion coefficient

[26] In Figures 4a and 4b we plotted the temporal behavior of the longitudinal dispersion coefficient given by the numerical simulations as well as the explicit expres-

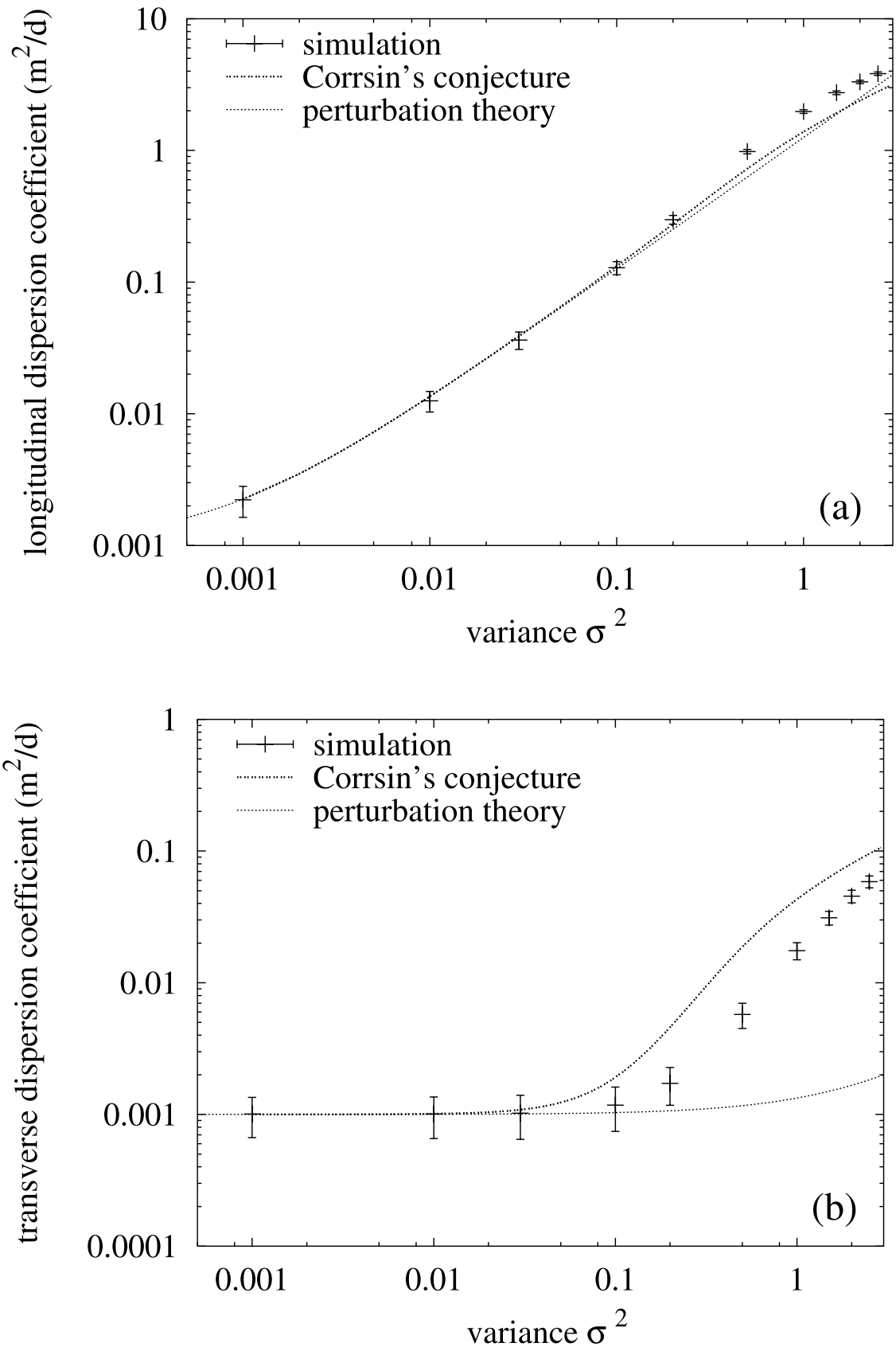

Figure 1. Asymptotic (a) longitudinal and (b) transverse dispersion coefficients as a function of the variance σ^2 for a local dispersion coefficient of $D = 0.001$ m^2/d in $d = 3$.

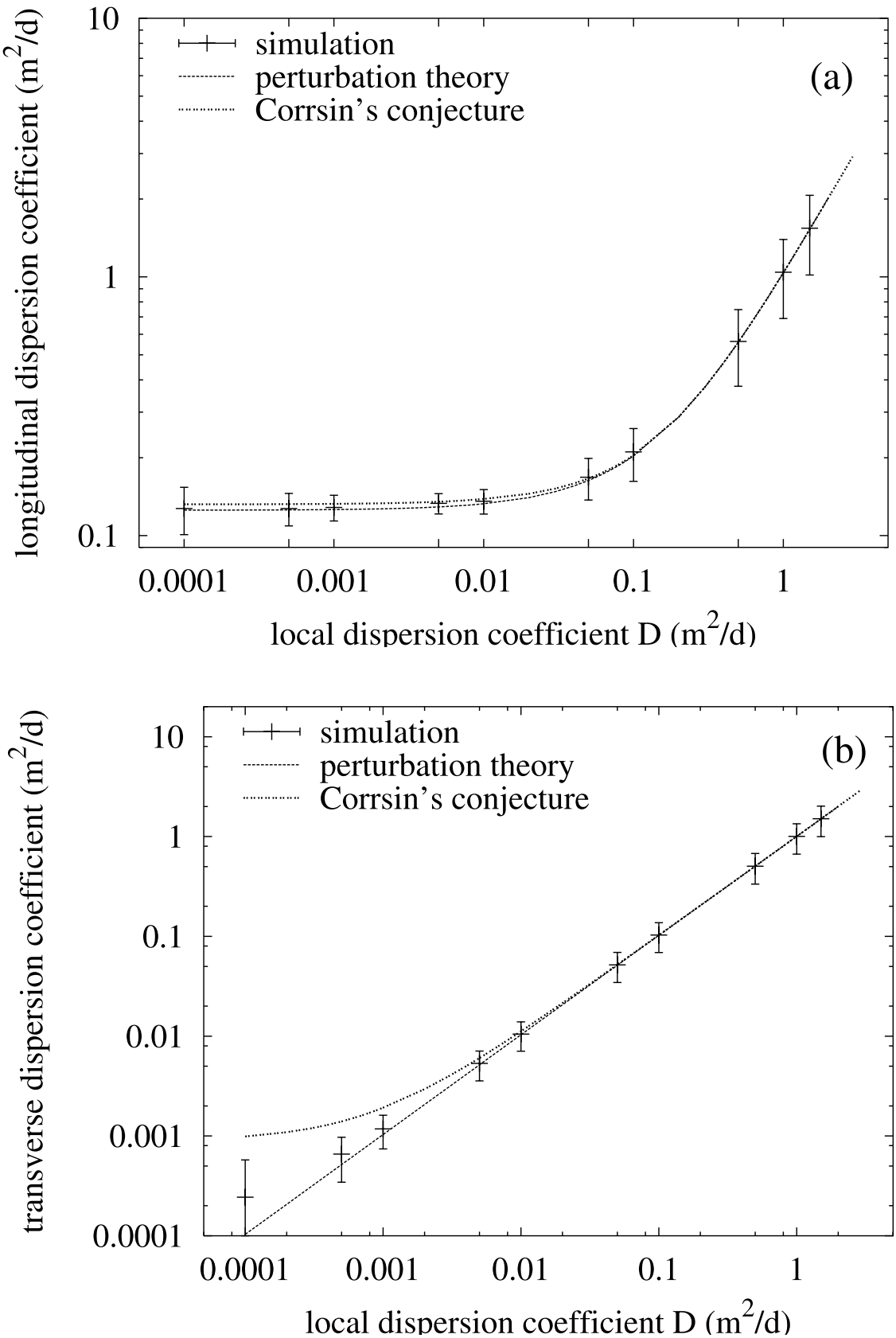

Figure 2. Asymptotic (a) longitudinal and (b) transverse dispersion coefficients as a function of the local dispersion coefficient D in $d = 3$ (with $\sigma^2 = 0.1$, $l = 1$ m and $\overline{u} = 1$ m/d).

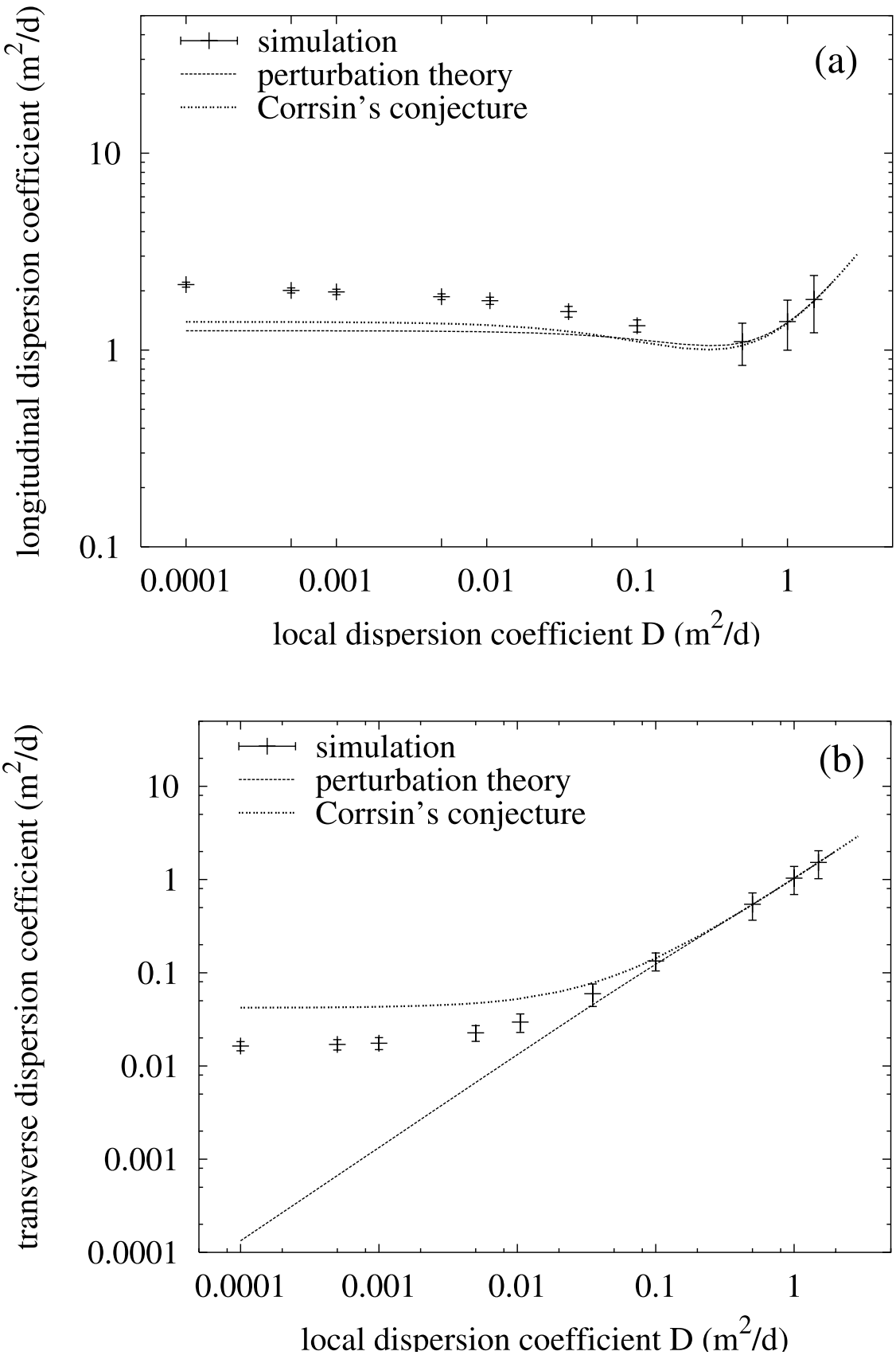

Figure 3. Asymptotic (a) longitudinal and (b) transverse dispersion coefficients as a function of the local dispersion coefficient D in $d = 3$ (with $\sigma^2 = 1$, $l = 1$ m and $\overline{u} = 1$ m/d).

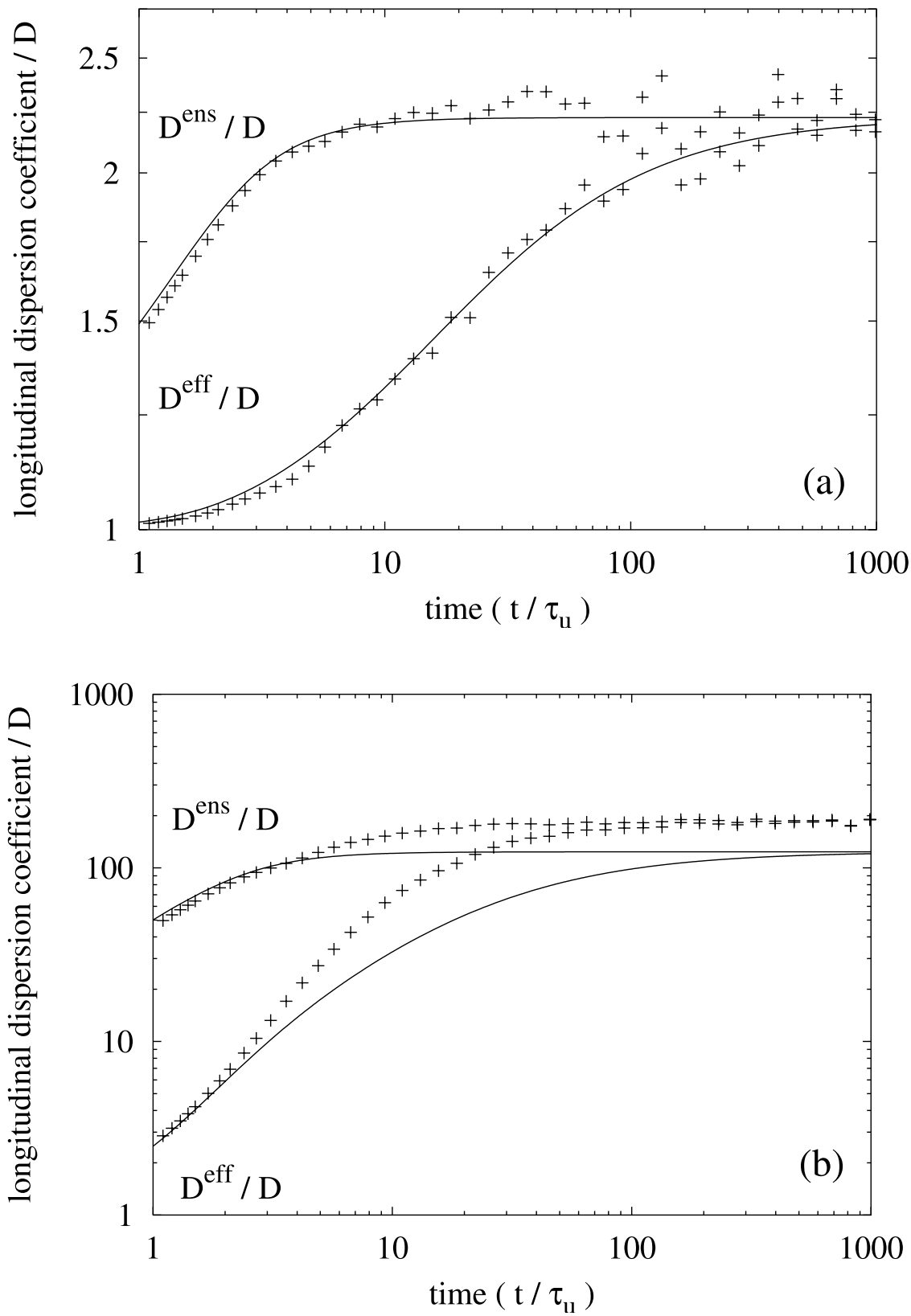

Figure 4. Temporal behavior of the longitudinal ensemble and effective dispersion coefficients normalized by D for $\epsilon = \tau_u/\tau_D = 0.01$, and the corresponding second-order expressions in $d = 3$ (with (a) $\sigma^2 = 0.01$ and (b) $\sigma^2 = 1$, $\overline{u} = 1$ m/d and $l = 1$m).

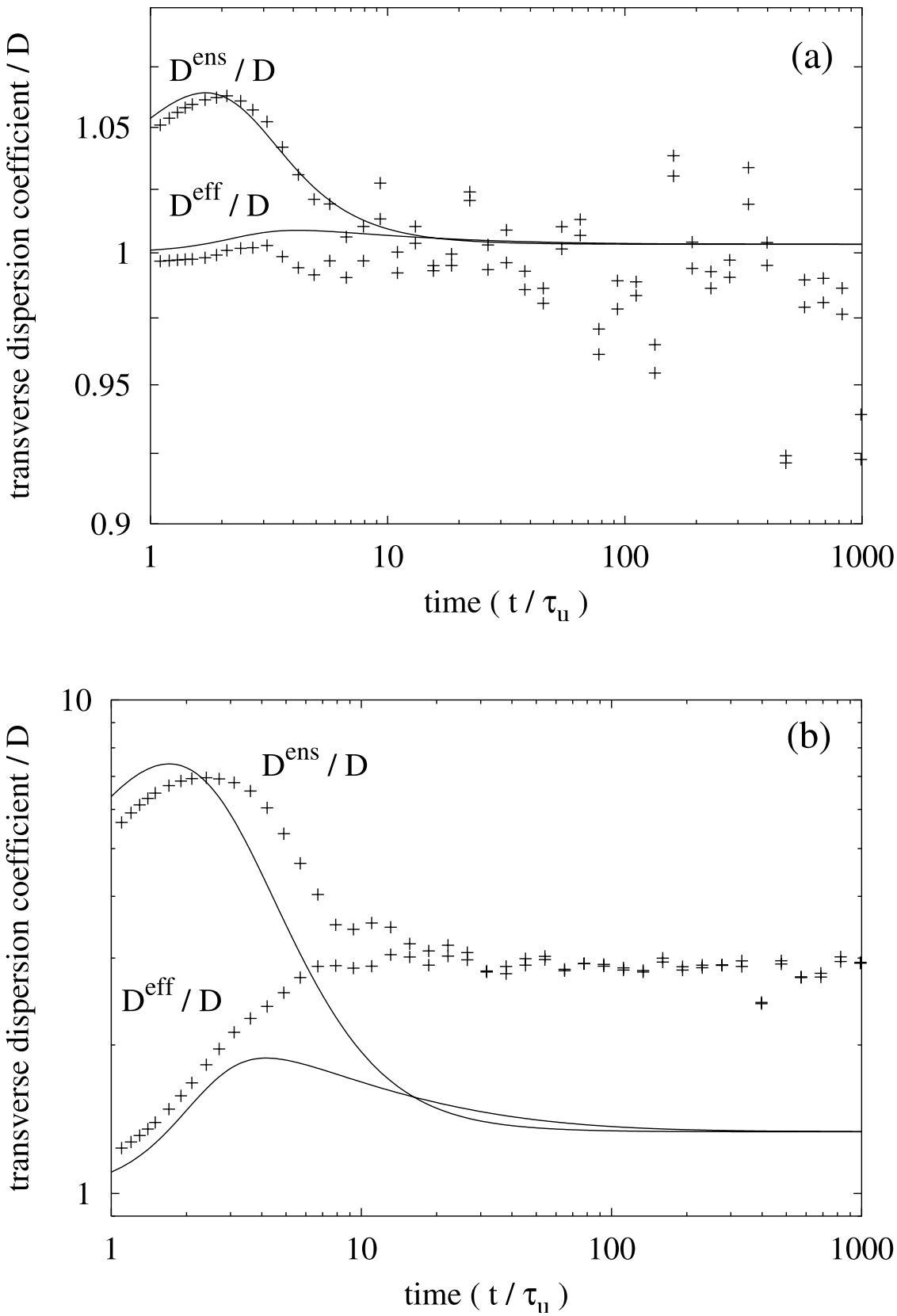

Figure 5. Temporal behavior of the transverse ensemble and effective dispersion coefficients normalized by D for $\epsilon = \tau_u/\tau_D = 0.01$, and the corresponding second-order expressions in $d = 3$ (with (a) $\sigma^2 = 0.01$ and (b) $\sigma^2 = 1$, $\overline{u} = 1$ m/d, $l = 1$ m).

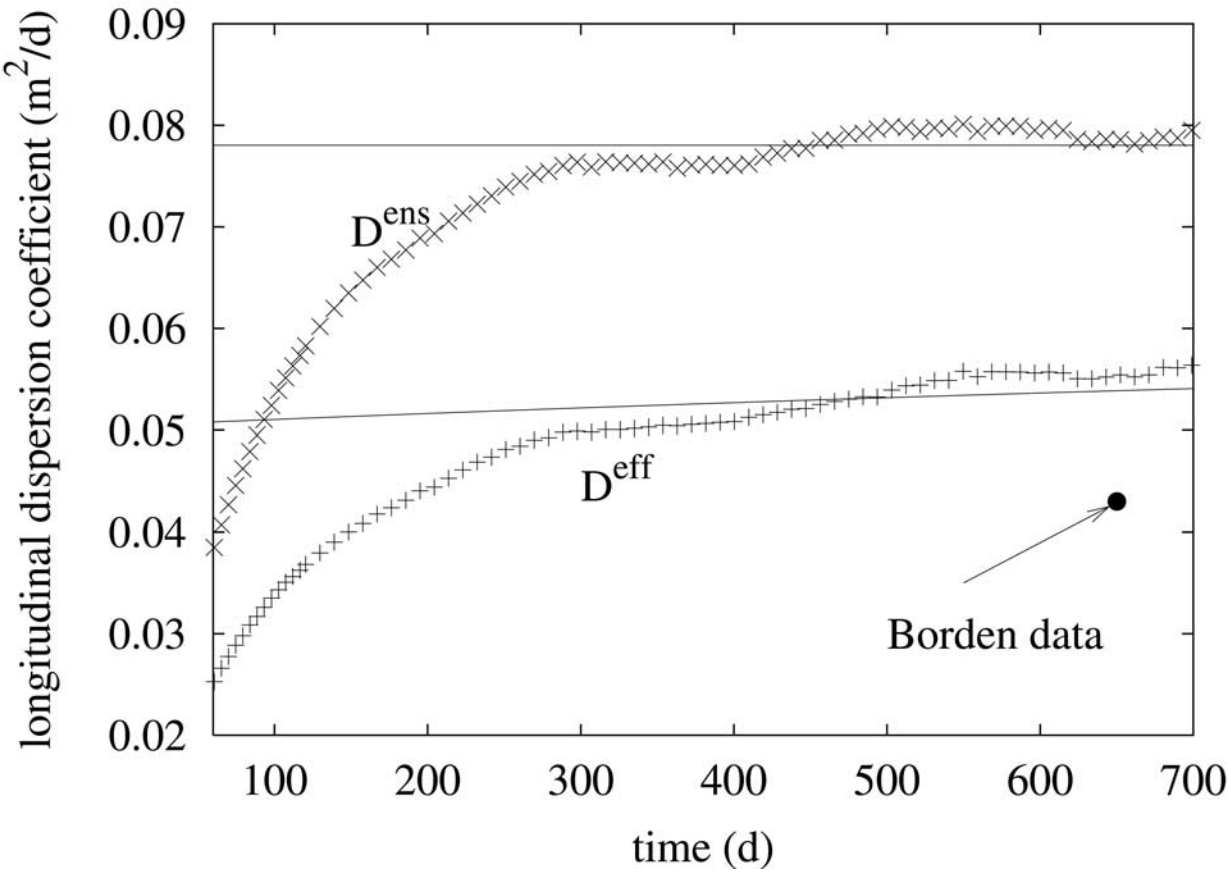

Figure 6. Effective and ensemble longitudinal dispersion coefficients for the Borden scenario compared to the expressions given by second-order perturbation theory.

sions derived from second-order perturbation theory given in paper 1 for variances of $\sigma^2 = 0.01$ and $\sigma^2 = 1$, respectively.

[27] For times larger than the dispersive timescale τ_D the effective and ensemble dispersion coefficients converge to the same asymptotic value. The characteristic difference between the ensemble and effective dispersion coefficients for finite times discussed in paper 1 in the context of second-order perturbation theory is confirmed very well by the simulation results. The effective dispersion coefficient, which reflects the dispersion properties of one typical realization of the medium evolves on the dispersive timescale τ_D. The ensemble quantity, in contrast, already reaches its asymptotic value on the much smaller advective timescale τ_u owing to contributions due to large sample to sample fluctuations of the center of mass of the solute cloud. Consequently the ensemble dispersion coefficient overestimates the dispersion in one typical realization of the medium remarkably within the intermediate time regime, $\tau_u \ll t \ll \tau_D$, which is relevant for many practical purposes. In realistic advection-dominated transport scenarios, the dispersive timescale τ_D is much larger than the advective timescale τ_u. In the Borden scenario, for example, the relevant dispersive timescale is of the order of 10^3 days while the advective timescale is of the order of 100 days, see e.g., paper 1. In this case, as we will see in the next section, the effective dispersion coefficient describes the measured data much better than the corresponding ensemble coefficient (see also paper 2). Furthermore, in the case that the solute interacts with the medium (e.g., adsorption, biodegredation), the transport behavior is very sensitive to the volume covered by the tracer. Using the ensemble dispersion coefficient to estimate the spreading of the solute for finite times leads to erroneous results.

[28] For small variances the behavior of the effective and ensemble dispersion coefficients agrees well with the behavior given by the explicit second-order perturbation theory expressions as illustrated in Figure 4a for $\sigma^2 = 0.01$. With increasing variance one observes pronounced deviations from the behavior given by second-order perturbation theory, see Figure 4b for the case $\sigma^2 = 1$. As already discussed for the asymptotic behavior of the dispersion coefficients, the long-time limit of the longitudinal dispersion coefficient is underestimated by the perturbation theory.

3.2.2. Transverse dispersion coefficient

[29] Figures 5a and 5b show the temporal behavior of the transverse dispersion coefficients for $\sigma^2 = 0.01$ and $\sigma^2 = 1$, respectively. We plotted the simulation data and the corresponding explicit second-order expressions given in paper 1. Due to the limited number of disorder realizations and the small absolute value of the dispersion coefficient the simulation data appear relatively noisy here. The fluctuations become smaller with an increasing number of disorder realizations. Again we notice a significant difference between the effective and the ensemble quantity

within the intermediate time regime $\tau_u \ll t \ll \tau_D$ while both quantities converge on the dispersive timescale. For small variances the second-order perturbation theory results agree with the simulation data as is illustrated in Figure 5a for $\sigma^2 = 0.01$. However, the behavior of the transverse dispersion coefficients changes considerably with increasing variance σ^2, see Figure 5b for the case $\sigma^2 = 1$. The effective dispersion coefficient evolves within the intermediate time regime and reaches its final macroscopic value on the dispersive timescale in agreement with many field findings which also yield a macroscopic transverse dispersion coefficient in contrast to the second-order results. On the advective time scale the behavior of the ensemble dispersion coefficient agrees with the prediction by second-order perturbation theory. For increasing times, however, it is underestimated significantly.

3.2.3. Borden scenario

[30] So far we have been investigating the situation of a point-like injection and isotropic disorder correlation. In the following we discuss a more realistic anisotropic aquifer situation as found at the Borden site (Ontario, Canada) [*Mackay et al.*, 1986; *Freyberg*, 1986]. For the simulations we use a source consisting of 40 particles per realization of the random flow field, which we choose from a Gaussian distribution (see paper 2). We use 2000 realizations of the Gaussian random field $\mathbf{u}(\mathbf{x})$ and 25 noise-realizations (The relatively small number is due to the limitation of computing time). The geostatistical data which we need as an input for the numerical simulations are summarized in paper 1 and 2. As is illustrated in Figure 6 the approximate analytical expressions given in paper 2 for the longitudinal effective and ensemble dispersion coefficients and the respective simulation data are in agreement in the time regime where the analytical approximation is valid, namely for $t \gg \tau_u = 85$ d. The significant difference between the effective and the ensemble dispersion coefficients is confirmed. The ensemble dispersion coefficient overestimates the data point considerably. The effective dispersion coefficient in contrast, which describes the dispersion in one single aquifer, agrees much better with the experimental findings.

4. Summary

[31] The objective of the numerical studies presented here was to complement and critically investigate the limitations of the analytical efforts given in the first two articles of the series [*Dentz et al.*, 2000a, 2000b]. We employed an efficient simulation method to investigate systematically the temporal behavior of the ensemble and the effective dispersion coefficients for solute transport in a heterogeneous flow field given by the linearized solution of the Darcy equation. We evaluated the asymptotic behavior of the longitudinal and transverse dispersion coefficients as a function of the variance σ^2 and as a function of the local dispersion coefficient D. Furthermore, we determined the full temporal behavior of the ensemble and effective dispersion coefficients.

[32] The results confirmed clearly the quantitative and qualitative difference between the effective and ensemble quantities, as predicted by the second-order perturbation theory results given in papers 1 and 2. For small values of the variance σ^2 the simulation data and the explicit expressions for the longitudinal dispersion coefficient given there agree extremely well. For the transverse dispersion coefficients the simulations resulted in values of macroscopic order of magnitude, in contrast to the predictions made by second-order perturbation theory. The self-consistent resummation of the perturbation series known as ''Corrsin's conjecture'' in the literature indeed predicts such a macroscopic value, but it actually overestimates the simulation data considerably. In passing, let us note that in similar simulations for a two-dimensional situation the conclusion would be completely different. In this case the simulations show that the transverse dispersion coefficient indeed is of microscopic order only, as predicted by the perturbation theory results, whereas the values derived from Corrsin's conjecture are completely erroneous (M. Dentz et al., Numerical studies of the temporal behavior of a solute cloud in a two-dimensional spatially varying flow field, submitted to *Stochastic Environmental Research and Risk Assessment*, 2002).

References

Ababou, R., D. B. McLaughlin, L. W. Gelhar, and A. F. B. Tompson, Numerical simulation of three-dimensional saturated flow in randomly heterogeneous porous media, *Transp. Porous Media*, *4*, 549–565, 1989.

Adams, E. E., and L. W. Gelhar, Field study of dispersion in a heterogeneous aquifer, 2, Spatial moment analysis, *Water Resour. Res.*, *28*, 3293–3308, 1992.

Attinger, S., M. Dentz, H. Kinzelbach, and W. Kinzelbach, Temporal behavior of a solute cloud in a chemically heterogeneous porous medium, *J. Fluid Mech.*, *386*, 77–104, 1999.

Bellin, A., P. Salandin, and A. Rinaldo, Simulation of dispersion in heterogeneous porous formations: Statistics, first-order theories, convergence of computations, *Water Resour. Res.*, *28*, 2211–2227, 1992.

Burr, D. T., and E. A. Sudicky, Nonreactive and reactive solute transport in three-dimensional heterogeneous porous media: Mean displacement, plume spreading, and uncertainty, *Water. Resour. Res.*, *3*, 791–815, 1994.

Chin, D. A., and T. Wang, An investigation of the validity of first-order stochastic dispersion theories in isotropic porous media, *Water Resour. Res.*, *28*, 1531–1542, 1992.

Dagan, G., Solute transport in heterogeneous porous formations, *J. Fluid Mech.*, *145*, 151–177, 1984.

Dagan, G., Time-dependent macrodispersion for solute transport in anisotropic heterogeneous aquifers, *Water Resour. Res.*, *24*, 1491–1500, 1988.

Dagan, G., *Flow and Transport in Porous Formations*, Springer-Verlag, New York, 1989.

Dagan, G., An exact nonlinear correction to transverse macrodispersivity for transport in heterogeneous formations, *Water Resour. Res.*, *30*, 2699–2705, 1994.

Dentz, M., Temporal behavior of transport parameters in heterogeneous porous media, Ph.D. dissertation, Univ. of Heidelberg, Heidelberg, Germany, 2000.

Dentz, M., H. Kinzelbach, S. Attinger, and W. Kinzelbach, Temporal behavior of a solute cloud in a heterogeneous porous medium, 1, Point-like injection, *Water Resour. Res.*, *36*, 3591–3604, 2000a.

Dentz, M., H. Kinzelbach, S. Attinger, and W. Kinzelbach, Temporal behavior of a solute cloud in a heterogeneous porous medium, 2, Spatially extended injection, *Water Resour. Res.*, *36*, 3605–3614, 2000b.

Drummond, I. T., S. Duane, and R. R. Horgan, Scalar diffusion in simulated helical turbulence with molecular diffusivity, *J. Fluid Mech.*, *138*, 75–91, 1984.

Fiori, A., Finite Peclet extensions of Dagan's solutions to transport in anisotropic heterogeneous formations, *Water Resour. Res.*, *32*, 193–198, 1996.

Freyberg, D. L., A natural gradient experiment on solute transport in a sandy aquifer, 2, Spatial moments and the advection and dispersion of nonreactive tracers, *Water Resour. Res.*, *22*, 2031–2046, 1986.

Gelhar, L. W., *Stochastic Subsurface Hydrology*, Prentice Hall, Old Tappan, N. J., 1993.

Gelhar, L. W., and C. L. Axness, Three-dimensional stochastic analysis of macrodispersion in aquifers, *Water Resour. Res.*, *19*, 161–180, 1983.

Honerkamp, J., *Stochastic Dynamical Systems*, VCH, New York, 1994.

Jaekel, U., and H. Vereecken, Renormalization group analysis of macrodispersion in a directed random flow, *Water Resour. Res.*, *33*, 2287–2299, 1997.

Kapoor, V., and P. K. Kitanidis, Concentration fluctuations and dilution in two-dimensionally periodic heterogeneous porous media, *Transp. Porous Media*, *21*, 91–119, 1996.

Kraichnan, R. H., Diffusion by a random velocity field, *Phys. Fluids*, *13*, 22–31, 1970.

Kraichnan, R. H., Diffusion of a passive-scalar and magnetic fields by helical turbulence, *J. Fluid Mech.*, *77*, 753–768, 1976.

Mackay, D. M., D. L. Freyberg, P. V. Roberts, and J. A. Cherry, A natural gradient experiment on solute transport in a sand aquifer, 1, Approach and overview of plume movement, *Water Resour. Res.*, *22*, 2017–2029, 1986.

Naff, R. L., D. F. Haley, and E. A. Sudicky, High-resolution Monte Carlo simulation of flow and conservative transport in heterogeneous porous media, 2, Transport results, *Water Resour. Res.*, *4*, 679–697, 1998.

Neuman, S. P., and Y.-K. Zhang, A quasi-linear theory of non-Fickian and Fickian subsurface dispersion, 1, Theoretical analysis with application to isotropic media, *Water Resour. Res.*, *26*, 887–902, 1990.

Risken, H., *The Fokker-Planck Equation*, Springer-Verlag, New York, 1984.

Rubin, Y., Stochastic modeling of macrodispersion in heterogeneous porous media, *Water Resour. Res.*, *26*, 133–141, 1990.

Salandin, P., and V. Fiorotto, Solute transport in highly heterogeneous aquifers, *Water Resour. Res.*, *34*, 949–961, 1998.

Schwarze, H., U. Jaekel, and H. Vereecken, Estimation of macrodispersion by different approximation methods for flow and transport in randomly heterogeneous media, *Transp. Porous Media*, *43*, 245–287, 2001.

Smith, L., and F. W. Schwartz, Mass transport, 1, A stochastic analysis of macroscopic dispersion, *Water Resour. Res.*, *17*, 351–369, 1980.

Tompson, A. F. B., and L. W. Gelhar, Numerical simulation of solute transport in three-dimensional, randomly heterogeneous porous media, *Water. Resour. Res.*, *26*, 2541–2562, 1990.

Zhang, Q., Transient behavior of mixing induced by a random velocity field, *Water Resour. Res.*, *3*, 577–591, 1995.

Zhang, Y., and J. Lin, Numerical simulations of transport of non-ergodic solute plumes in heterogeneous aquifers, *Stochastic Hydrol. Hydraul.*, *12*, 117–140, 1998.

Zhang, Y.-K., and S. P. Neuman, A quasi-linear theory of non-Fickian and Fickian subsurface dispersion, 2, Application to anisotropic media and the Borden site, *Water Resour. Res.*, *26*, 903–913, 1990.

S. Attinger and W. Kinzelbach, Institut für Hydromechanik und Wasserwirtschaft, Eidgenössisch Technische Hochschule Zürich, 8093 Zürich, Switzerland. (attinger@ihw.baum.ethz.ch; kinzelbach@ihw.baum.ethz.ch)

M. Dentz, Department of Environmental Science and Energy Research, Weizmann Institute of Science, 76100 Rehovot, Israel. (marco.dentz@weizmann.ac.il)

H. Kinzelbach, Institut für Theoretische Physik, Universität Heidelberg, Philosophenweg 19, 69120 Heidelberg. (kibach@tphys.uni-heidelberg.de)